

Design and Development of Three-Bladed Propeller for Micro Air Vehicles

Prathapanayaka R., Vinod Kumar N., Santhosh Kumar S., Veera Sesha Kumar, and Krishnamurthy S. J.
Propulsion Division, CSIR – National Aerospace Laboratories, Bangalore, India

Abstract—CSIR-National Aerospace Laboratories (CSIR-NAL) is having a major program on development of Micro Air Vehicles (MAV) for civil, surveillance, and defense use. Under this program, MAV components development has been undertaken in various divisions of NAL. Propulsion system for one of the configurations of NAL MAV having fixed wing is battery-driven miniature motor and mini propellers. Efficient propulsion system plays a major role in deciding the endurance, payload, and maneuverability of MAV's. Design of efficient propellers for these classes of vehicles is a challenging task because of their lower operating Reynolds number as well as conservative power utilization to enhance the endurance. Earlier, 2-bladed, fixed pitch, variable speed, 6-inch diameter propellers with different plan form has been carried out and reported. The present requirement is for 3-bladed, fixed pitch, variable speed mini propellers to augment thrust within the geometrical constraints as envisaged in the design of two-bladed propellers. To meet the mission requirements, design of three-bladed, fixed pitch, variable speed mini propellers were carried out using minimum induced loss method, and Eppler-193 airfoil is used in the design in view of its higher lift to drag ratios at low Reynolds numbers. This resulted in slight penalty on weight as well as power consumption and reduced noise level. Propeller CAD model is generated using SOLID WORKS and used for analysis as well as for fabrication. Performance estimation for this propeller is carried out using blade element momentum theory and ANSYS FLUENT. Fabrication of this propeller is carried out using three methods namely rapid prototype (RPT) using poly carbonate and conventional vacuum casting using poly urethane material and CFRP material with conventional casting using aluminum mold. The overall performance parameters like thrust, propulsive efficiency and motor power are evaluated for CFRP propeller and tested at uninstalled condition. Overall performance of the propellers is evaluated at MAV Aerodynamics Research Tunnel (MART), CSIR-NAL for different wind velocities and propeller rotational speeds in uninstalled conditions. This paper brings out the work carried out on design, development and testing of three-bladed miniature propeller for MAVs and its analysis using computational tools at propulsion division, CSIR-NAL.

Keywords—MAV propellers, propeller aerodynamics, blade element momentum theory, propeller testing.

NOMENCLATURE

| | |
|-------------|----------------------------------|
| A | area, m ² |
| B | number of blades |
| C_d | coefficient of drag |
| C_l | coefficient of lift |
| C_p | coefficient of power |
| C_q | coefficient of torque |
| C_t | coefficient of thrust |
| F | Prandtl's circulation correction |
| D | propeller diameter, m |
| dT | elemental thrust, N/m |
| dQ | elemental torque, N.m/m |
| J | advance ratio |
| N | rotational speed, rpm |
| P | power, Watt |
| Q | torque, N.m |
| R | radius of propeller, m |
| Re | Reynolds number |
| rh | radius of hub, m |
| T | thrust, N |
| V | flight speed, m/s |
| a | axial inflow factor |
| a' | tangential inflow factor |
| c | blade chord, m |
| c/R | chord to radius ratio |
| f | vortex sheet spacing parameter |
| f_{hub} | hub loss correction factor |
| f_{tip} | tip loss correction factor |
| n | propeller rotational speed, rps |
| p | static pressure, Pa |
| r | radius at section, m |
| Ω | angular velocity (rad/sec) |
| α | angle of attack, degree |
| β | blade angle (twist), degree |
| \emptyset | helix angle, degree |
| ρ | density, kg/m ³ |
| η | efficiency |

ABBREVIATIONS

| | |
|----------|---|
| MAV | Micro Air Vehicle |
| CFRP | Carbon Fiber Reinforced Plastic |
| CSIR | Council of Scientific and Industrial Research |
| NAL | National Aerospace Laboratories |
| MART | MAV Aerodynamics Research Tunnel |
| CSMST | Centre for Societal Missions and Special Technologies |
| DRDO | Defence Research and Development Organisation |
| ADE | Aeronautical Development Establishment |
| NP-MICAV | National Programme on Micro Air Vehicles |
| ABS | Acrylonitrile butadiene styrene |
| RNG | Renormalization Group |

I. INTRODUCTION

WORLDWIDE, there is a serious interest in development of micro and nano scale air vehicle development for surveillance and defense application. Various research institute, universities, and industries have been involved in development of miniaturized and efficient components for these classes of vehicles [1]. National Aerospace Laboratories, one of the premier research institute for aerospace under Council of Scientific and Industrial Research (CSIR) have been involved in development of micro air vehicles for the past five years. CSIR-NAL under the sponsorship of DRDO-ADE, Bangalore has developed Black Kite (300 mm wing span), GOLDEN HAWK (450 mm wing span) and PUSHPAK (450 mm wing span) micro air vehicles. All these MAVs are of fixed wing type and driven by electric propulsion system. Various divisions of CSIR-NAL are involved in component-wise development of MAV. The propulsion system of NAL MAVs is battery driven electric brushless motor and propellers. There is always a scope to improve the performance of MAV by optimizing the design of propulsion system. Propulsion division of CSIR-NAL is involved in the design and development of miniature propellers for the above said MAVs and has designed and developed a two-bladed, fixed pitch, six inch diameter propeller with a peak propulsive efficiency of 72% for Black Kite [2]–[7]. The present requirement is to augment thrust and geometrical constraints used earlier with a slight penalty on weight as well as power consumption, expected to be at reduced noise has been carried out to meet the mission requirements. Design and development of three-bladed, fixed pitch, variable speed, and six inch diameter miniature propellers and its analysis using computational tools will be discussed in the proceeding sections of this paper.

II. METHODOLOGY

The design of mini propellers for micro air vehicles requires a priori thrust or power, propulsive efficiencies, mission requirements, geometrical constraints, and materials. Propulsive efficiency depends on the efficiencies of the airfoil's having high lift to drag ratios at operating Reynolds number and flight velocities. At the same time it depends on how the airfoils are stacked and on its chord distribution along the span for the power availability to get maximum thrust.

Propeller blade planform which is described by its chord and twist distribution is designed using minimum induced loss method [8] by prescribing the thrust or power. The present configuration of micro air vehicle demands thrust to weight ratio of 0.6 at take-off condition. A computer program “NALPROPELLER code” is developed on MATLAB platform, using minimum induced loss method and BEMT [10] is used to generate propeller blade plan-form and overall performance parameters like coefficients of thrust, torque, power and efficiencies at different advance ratios of the propellers. However drag polar of the airfoil's need to be evaluated separately using XFLR5 for different flight conditions, and used as input in to the “NALPROPELLER code”. Three-dimensional model of the propellers is generated using SOLIDWORKS. The effort to realize the product with good structural integrity by using CFRP material, machining a mold having three dimensional contour using 3-axis NC milling machine is accomplished. The CFRP propeller is evaluated for different propeller rotational speed and wind velocities using customized propeller test setup procured from M/s MAGTROL SA, Switzerland.

TABLE I DESIGN SPECIFICATION

| Specifications for NAL MAV | | Base line requirements of propellers | |
|----------------------------|-------------------------|--------------------------------------|---|
| Name | Black Kite | Propeller Diameter | 152mm (Aprox 6") |
| Type | Fixed Wing | Pitch | 127 mm (5"), Fixed |
| Span | 300 mm | Speed N | 6000 to 10,000 rpm |
| Weight | 300g | No of blades | 3 |
| Cruise Speed | 10-15 m/s | Type & Version | Tractor, NP3B6050 |
| Operation Altitude | 30-100 m AGL | Tip Speed | 47.75m/s to 79.58m/s |
| Endurance required | 30 mins | Advance ratio | 0.7894 to 0.473 |
| Launch | Hand | Design thrust at cruise | 80 grams (Take-off thrust: 180 grams) |
| Recovery | Soft landing | Efficiency | Better than 70 % |
| Mission range | > 2 km | Profiles used | NACA66-021(up-to r/R = 0.3), Eppler-193 (r/R 0.3-1.0) |
| Mission payload | Miniature Colour Camera | Material | CFRP |
| | | Weight of propeller | 6 grams |

III. PROCEDURE

The broad specification of NAL developed MAV Black-Kite (**Figure 1**) and base line requirements of propellers for its variants are given in **TABLE I**.

A. Design and BEMT Analysis

The design and analytical performance estimation of propeller is an iterative and lengthy process. In view of this, an in-house computer program “NALPROPELLER code” is

developed using MATLAB where in, the design details and overall performance parameters could be viewed in multiple windows simultaneously. This code is based on minimum induced loss method [8] to obtain the propellers blade plan form, and combined with blade element momentum theory. NALPROPELLER code is extensively used for the analytical design and performance estimation of the propeller in the present work. From baseline specifications, the propeller plan form is obtained using NALPROPELLER code for maximum takeoff thrust of 180 grams. Low Reynolds number airfoils such as Eppler 387, Eppler 193, NACA 4412, are used in evaluating its drag polar through commercially available computational tools like XFLR5, ANSYS, and its comparative studies has been carried out and reported [2]. Eppler 193 is found to be more suitable candidate having lift to drag ratio around 35 at the operating Reynolds number for the present application and also, in view of experimental values, [12] are available elsewhere.



Figure 1 Black Kite MAV

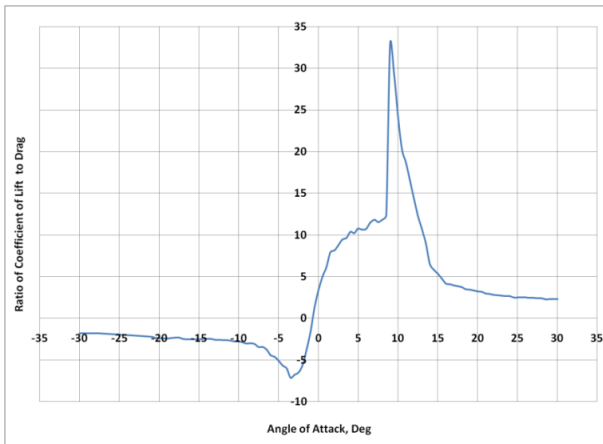


Figure 2 Coefficient of lift to drag ratio vs. angle of attack at Re, 45000, XFLR5

Eppler 193 airfoil is used for most of the portion, and NACA 66-021 airfoil is used at the hub region of the propeller blade to provide sufficient strength. Propeller operating Reynolds number is close to 45,000 based on the chord at 75 % radius and relative velocity of the flow over a propeller blade operating at rotational speed of 8000 rpm and cruise flight velocity of 12 m/s. **Figure 2** shows the drag polar at propeller operating Reynolds number of 45,000 and Ncrit value of 9 is obtained from XFLR5.

The propellers blade plan form obtained from NALPROPELLER code is shown in **Figure 3** and **Figure 4**.

Figure 5 shows the velocity and force vector diagram for a particular section of the propeller. The elemental values of thrust, power and torque are evaluated using blade elemental momentum theory using the drag polar obtained from XFLR5. The elemental thrust and torque are given by

$$\text{Elemental thrust: } dT = 4\pi\rho r V_\infty^2 (1+a) a' F dr \quad (1)$$

$$\text{Elemental torque: } dQ = 4\pi\rho r^3 \Omega V_\infty (1+a) a' F dr \quad (2)$$

where Prandtl hub and tip loss factor:

$$F = \frac{2}{\pi} \cos^{-1} e^{-f}$$

$$f_{hub} = \frac{B}{2} \frac{r - R_{hub}}{r \sin \phi}$$

$$f_{tip} = \frac{B}{2} \frac{R - r}{r \sin \phi}$$

axial inflow factor:

$$a = \left[\frac{4F \sin^2 \phi}{\sigma(C_1 \cos \phi - C_d \sin \phi)} - 1 \right]^{-1}$$

tangential inflow factor

$$a' = \left[\frac{4F \sin \phi \cos \phi}{\sigma(C_1 \sin \phi - C_d \cos \phi)} + 1 \right]^{-1}$$

$$\tan \phi = \frac{V_\infty (1+a)}{\Omega r (1-a')}$$

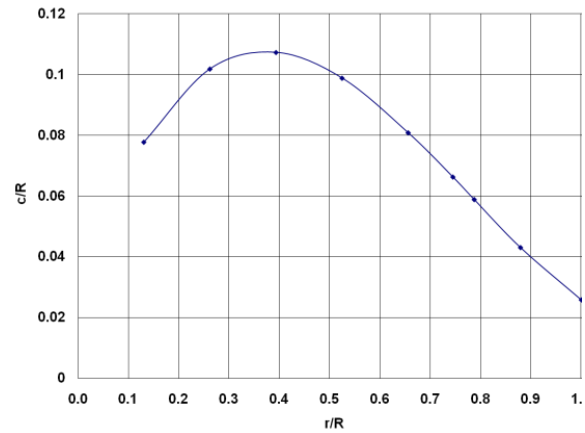


Figure 3 Chord distribution along blade span

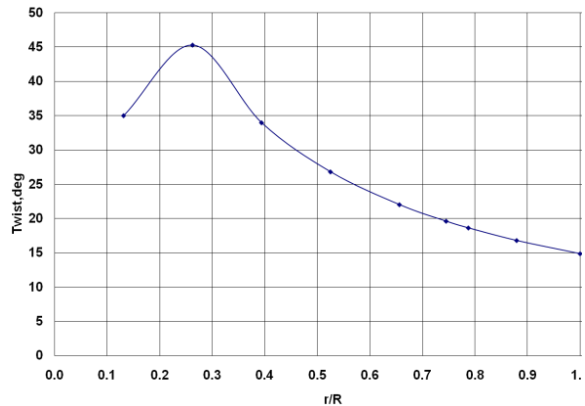


Figure 4 Twist distribution along blade span

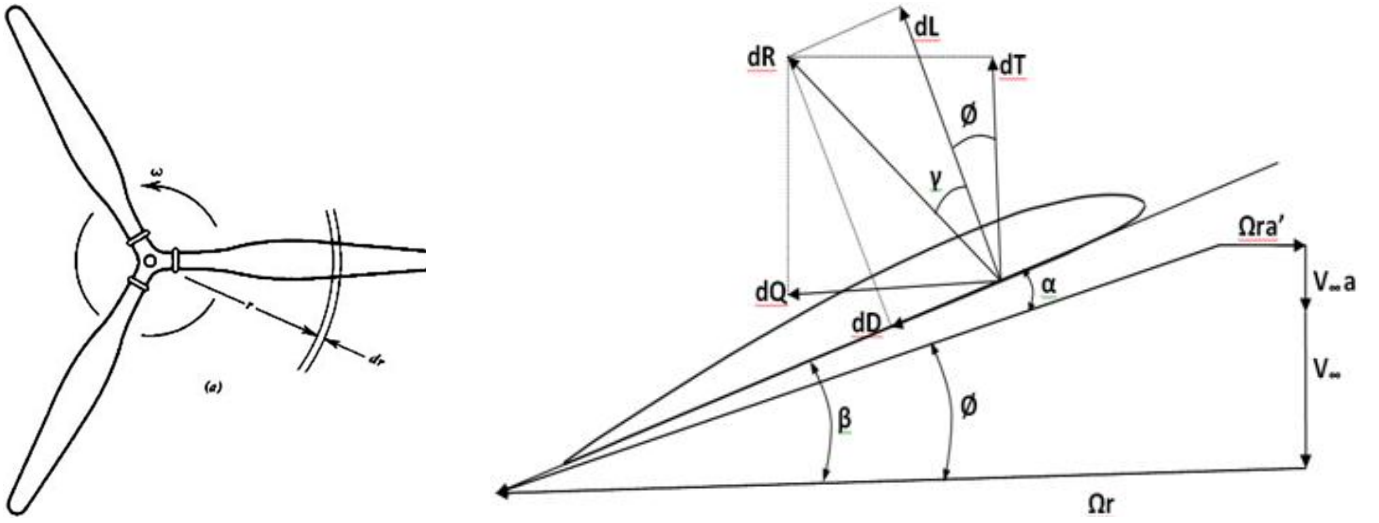


Figure 5 Aerodynamic forces over a blade element of the propeller

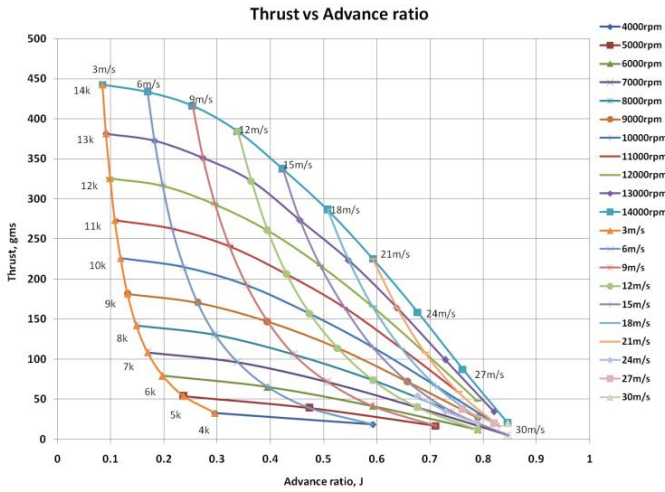


Figure 6 Carpet plot of thrust vs. advance ratio

The overall thrust force and torque of a blade can be obtained by integrating dT and dQ over the radius R and multiplying them with number of blades as given by (3) and (4).

$$T = B \int_{rh}^R dT \, dr \quad (3)$$

$$Q = B \int_{rh}^R dQ \, dr \quad (4)$$

Thrust coefficient: $C_t = \frac{\text{Thrust}}{\rho n^2 D^4} \quad (5)$

Power coefficient: $C_p = \frac{\text{Power}}{\rho n^3 D^5} \quad (6)$

Propulsive efficiency: $\eta = \frac{C_t}{C_p} J \quad (7)$

where

$$J = \frac{V_\infty}{nD}$$

NALPROPELLER code calculates all the performance coefficients as explained above, and these results can be viewed in multiple windows simultaneously. The elemental values of thrust, power, and torque are integrated over a span of the propeller blade using Simpson's one-third rule to obtain the total values of thrust, power, and torque.

Figure 6 shows the carpet plot and it provides thrust, propeller rotational speed, and flight velocity versus advance ratios. The blade plan form is from the NALPROPELLER code is used for CAD modeling using SOLID WORKS software. The CAD model of the propeller shown in Figure 7 is further used in CFD analysis, mold machining and propeller casting.

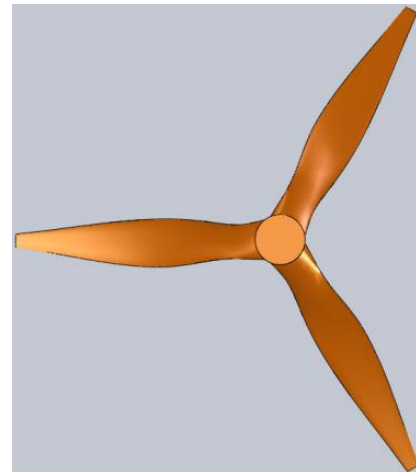


Figure 7 Propeller CAD model

B. 3D CFD Analysis

Flow domain and mesh over the propeller blade is created using GAMBIT software as shown in **Figure 8**. A truncated cone-like domain of upstream length is 3 times and downstream length is 10 times the diameter of propeller is created over the propeller. The domain shape and size is created in such way that total grid size is kept at minimum and also a domain boundary does not influence the flow near the propeller region. A cylindrical domain, slightly bigger than the size of the propeller, was created in order to simulate the flow with propeller in rotation, and 1.83 million tetrahedral grids were created over the propeller domain as shown in **Figure 8**. Finely spaced “tri pave” mesh as shown in **Figure 9** is generated over the surface of the propeller blades to closely approximate the airfoil geometry and near accurate estimation of the aerodynamic forces acting over the propeller blade surfaces.

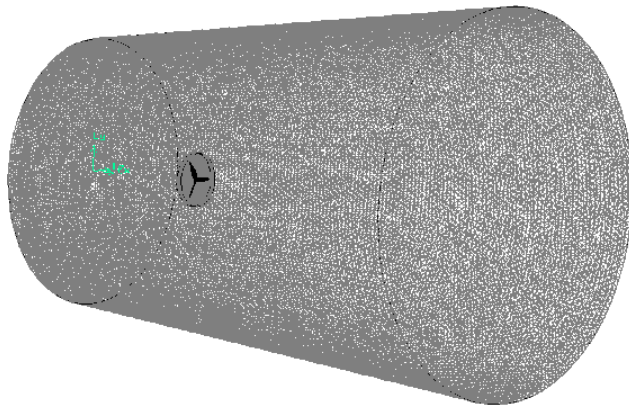


Figure 8 Tetrahedral grids (1.8 Million)

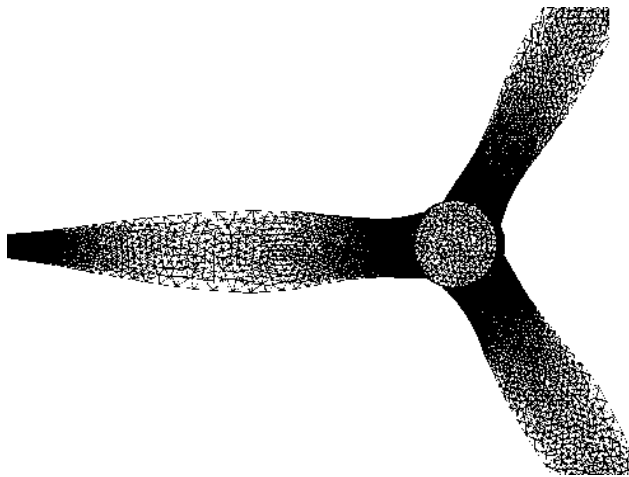


Figure 9 Tri-pave mesh over the propeller blade surface

3D CFD analysis is carried out using ANSYS FLUENT 6.3 to estimate the propeller thrust and torque at various operating condition of the MAV. Steady state, pressure-based solver with RNG k- ϵ turbulence model is used for the analysis. The flow is considered as incompressible and with local density is used in the analysis. RNG k- ϵ is a low Reynolds number turbulence model used for the flows encountering swirl, separation, and vorticity. The flow is considered to be converged at 10^{-4} and also the residual values are constant over few hundred iterations.

Grids dependency study is carried out using tetrahedral grids of 0.6, 1.83 and 3.9 million with RNG k- ϵ turbulence model. It is observed that 1.83 million grids give near accurate values.

The wall y plus values over the propeller blades are ranging from 30 to 60. **Figure 10** and **Figure 11** show the axial velocity contour and path lines colored with velocity magnitude at 8000 rpm and 12 m/s respectively.

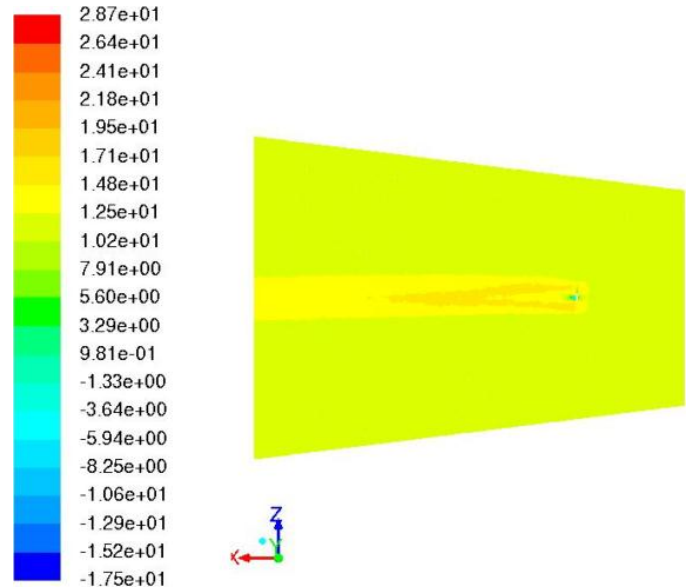


Figure 10 X-Velocity contour at 8000 rpm and 12 m/s

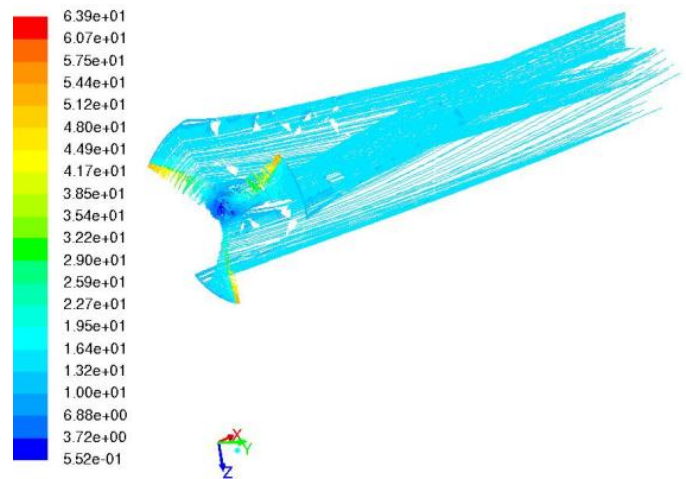


Figure 11 Path lines colored with velocity magnitude

C. Structural Analysis

Structural analysis for static and dynamic conditions are necessary for the structural integrity of the propellers; hence detail stress analysis has been carried out using ANSYS WORKBENCH, VERSION 14.5 [13] available at Propulsion division of NAL. The load distribution is evaluated from blade element momentum theory [14]. The CAD model of the propeller is taken from the above & imported into ANSYS WORKBENCH, finite element software. Solid element mesh generated using AUTOMESH feature in ANSYS. Tetrahedral mesh, nodes of 434855, elements of 285780, average cell aspect ratio of 2 and average skewness of 0.24 is used. The

static nonlinear analysis is carried out for the maximum speed of 12000 RPM at free stream wind velocity of 12 m/s with CFRP material, material data; boundary condition, thrust distribution and angular velocity are inputs. Stress analysis is carried out using non-linear geometric option. This option includes stress relief obtained due to centrifugal force over thrust. **TABLE II** shows the material properties, rotational speed and air load at constant free stream velocity of 12 m/s. **Figure 12(a)**, **Figure 12(b)**, **Figure 12(c)**, **Figure 12(d)**, and **Figure 12(e)** show von-Mises stresses, variation of radial stress along the span, radial displacement and two views of axial displacement of propeller blade respectively. The analysis show that the maximum bending stress and von-Mises stress are of the order of 14 MPa at r/R of 0.45 on suction surface and is well within the ultimate tensile strength of the material analyzed. The maximum tensile stress in the span wise direction occurs in the same location. The maximum displacement occurs at the propeller blade tip is in the order of 0.15 mm.

TABLE II MATERIAL PROPERTIES [15]

| Material | Carbon Fibre Reinforced Polymer |
|--|---|
| Density, gm/cm ³ | 1.6 |
| Youngs modulus (E), MPa Fabric @ 0° | 70 x 10 ⁶ |
| Shear Modulus (G), MPa | 5 x 10 ⁶ |
| UTS, MPa, Fabric @ 0° | 600 |
| Poissons ratio | 0.10 |
| Rotational speed | 12000 rpm, (Angular velocity 1256 radians per sec) |
| Air load, N | 1.4153N applied at a distace of 19 mm from the tip ($\frac{3}{4}$ of radius from axis). |

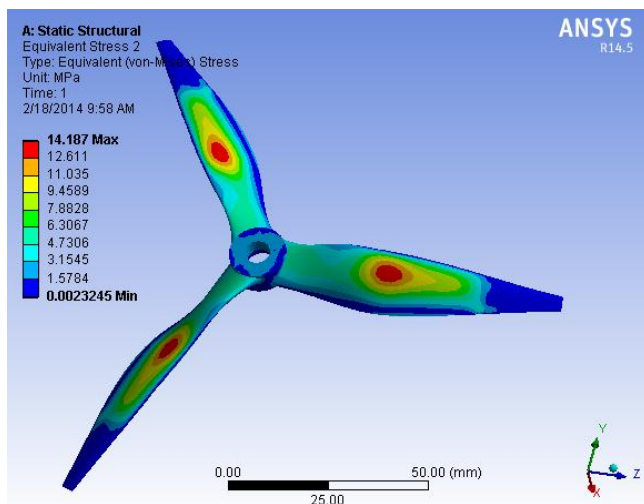


Figure 12(a) von-Mises stresses with aerodynamic force applied at $\frac{3}{4}$ th radius

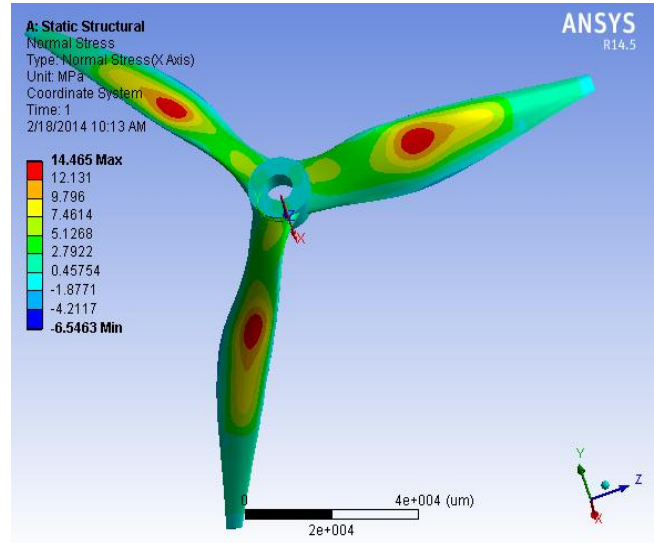


Figure 12(b) Variation of radial stress along the span

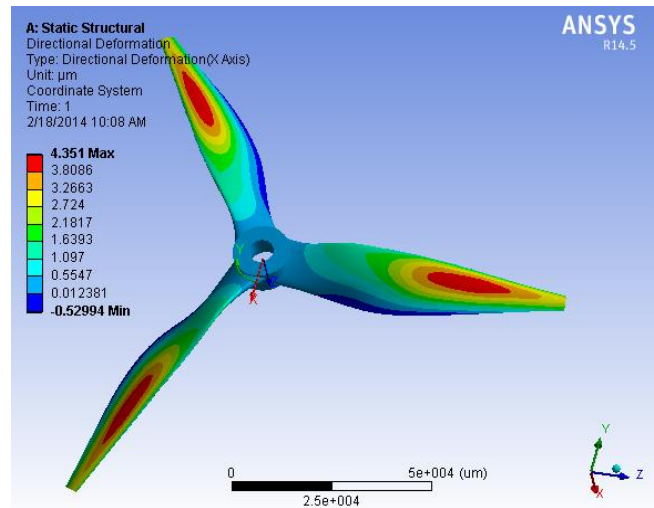


Figure 12(c) Radial displacement

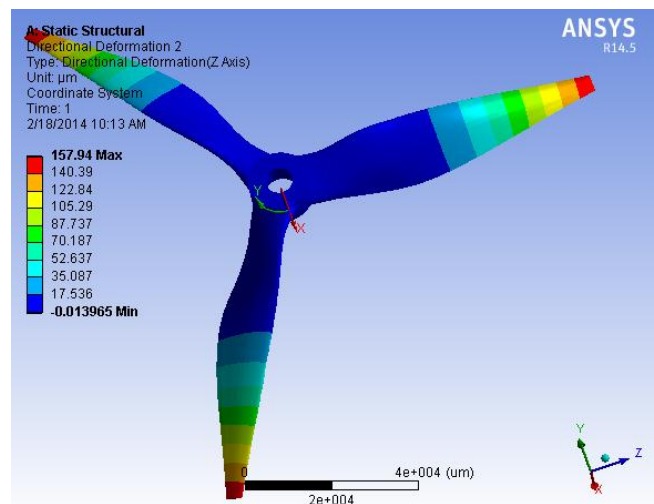


Figure 12(d) Axial displacement (front view)

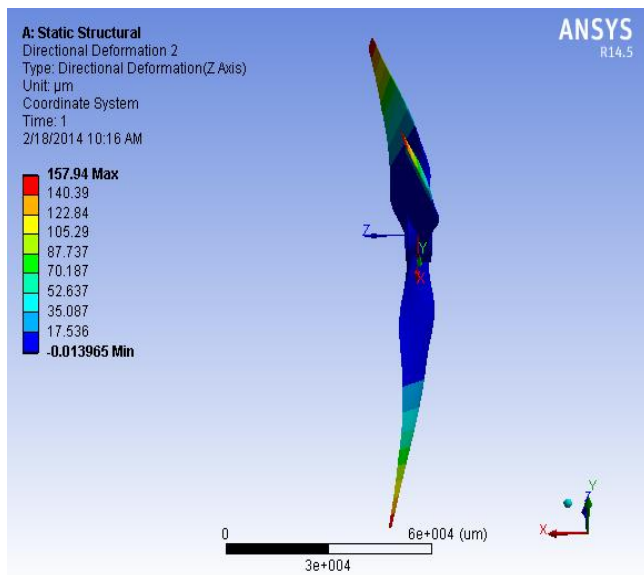
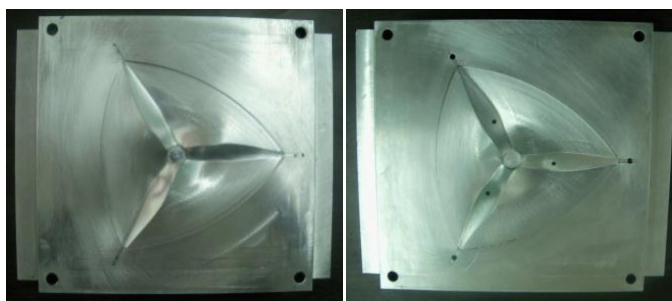


Figure 12(e) Axial displacement (side view)

D. Propeller fabrication

Propellers are fabricated from three different process namely RPT using poly carbonate, vacuum casting using poly urethane material, and injection molding using carbon fiber reinforced plastic (CFRP). In RPT method, the CAD model of propeller is used in RPT machine to fabricate the propeller using polycarbonate. In vacuum casting process, the propeller fabricated by RPT method is used as master propeller. Using this master propeller, silicon rubber mold is created. Finally, poly urethane material is used to obtain the propeller through vacuum casting process. However, propellers fabricated in these methods have limited structural integrity, accuracy and prone to failure during landing of MAVs. In later case, aluminum alloy mold is machined using CAD model, and three axes NC milling machine is used. The machined mould is as shown in **Figure 13**. Casted propellers using this process showed blow holes within the propeller blade, which is observed during testing. Further, it is rectified by allowing pressurized resin in to the mold under controlled environment. These propellers are statically balanced by trial & error method using TF top flite precision magnetic balancer [11], wherein floating shaft is suspended by two powerful ceramic-8 magnets. The propeller obtained through injection molding using CFRP material shows good structural integrity and accuracy. The CFRP propeller fabricated is as shown in **Figure 14**.



Top mold

Bottom mold

Figure 13 Aluminum molds



Figure 14 CFRP Propeller

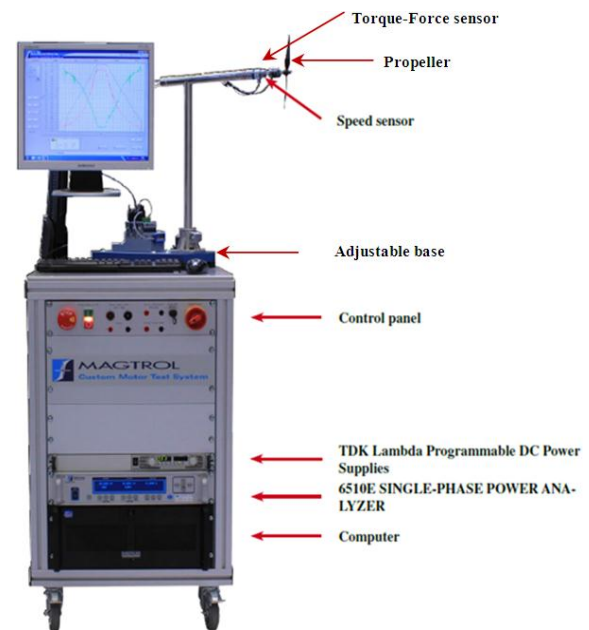


Figure 15 MAGTROL Customized Propeller test setup

E. Wind tunnel testing

The propeller performance is evaluated using MAGTROL customized propeller test set up [9] as shown in **Figure 15**. The major parameters measured using this test setup is thrust, torque, and propeller rotational speed simultaneously. Torque and thrust are measured by a combined Torque-Force sensor of maximum range 0.5 N.m and 50 N respectively. Torque-Force sensors have Accuracy class 1, 0.2 % v.E (Excitation voltage). The propeller is driven by an out runner brushless motor. An electronic speed controller (ESC) is used to control the speed of the motor. The propeller, motor, Torque-Force sensor and ESC are mounted on a horizontal bar which is supported by vertical bar mounted on an adjustable base. An optical infrared speed sensor is mounted on the horizontal bar in parallel to the axis and the sensor facing the propeller approximately 35 mm away and parallel to the main axis as well as 5 mm away from the propeller plane of rotation. The measured data are acquired by a compact NI DAQ system. The control panel unit consists of programmable DC power supply, single phase power analyzer, GPIB interface, computer, monitor, keyboard and its controls to

operate the test setup. During wind tunnel testing the adjustable base along with the DAQ cards and sensors is mounted inside the test section and the cabling are routed out of the tunnel to the control panel unit. Test cycle for various propeller rotational speeds and wind velocities is defined by time steps and throttle percentage.

Figure 16 shows the typical logged data obtained from the propeller test setup. Other than steady state data, the appearing few noise signals are from fluctuations in wind velocities and also could be from overall structural system. Atmospheric pressure and temperature are recorded for use in evaluating the propeller performance parameters. Post processing of data is carried out offline to present in most generic format of propulsive system.

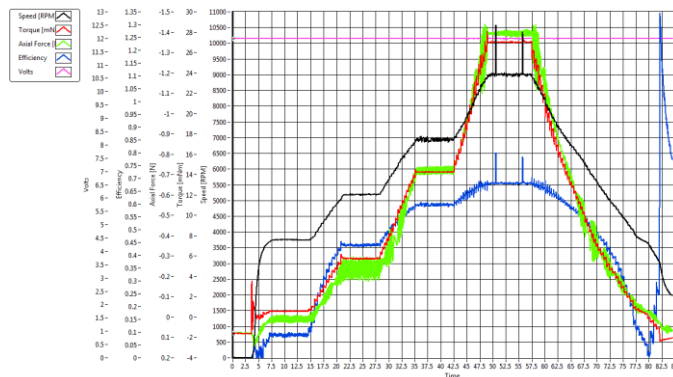


Figure 16 Typical plot of simultaneous data logged during propeller testing

IV. RESULTS AND DISCUSSIONS

The propeller overall performance parameter like coefficients of thrust, power and efficiency are evaluated using experimental results from wind tunnel testing with that of computed values from ANSYS FLUENT and NALPROPELLER code. **Figure 17** shows coefficient of thrust versus advance ratios at uninstalled conditions. The computed values of coefficients of thrust and power are slightly lower than the wind tunnel results. The difference between computed values of coefficient of thrust and wind tunnel values increases with increase in advance ratios, and more predominant beyond advance ratios of 0.55. A better agreement prevails in the operating range of advance ratios of 0.45 to 0.6. However, computed values from ANSYS-FLUENT are better comparable with that of experimental results in comparison to NALPROPELLER code. The lower prediction of thrust coefficient at higher advance ratios could be due to three dimensional effects which are not accounted in the NALPROPELLER code at present.

Figure 18 and **Figure 19** show coefficient of power and propulsive efficiencies versus advance ratio at uninstalled conditions respectively. Though the trend of predictions is in good agreement, measured power is slightly higher than the predictions. The torque, thrust, and speed are simultaneously measured using the MAGTROL test set up. Under prediction of coefficient of power in NALPROPELLER code may be due to severe uncertainty in estimating the drag polar, using potential

flow code as well as its operating Reynolds numbers along the span in 2D environment.

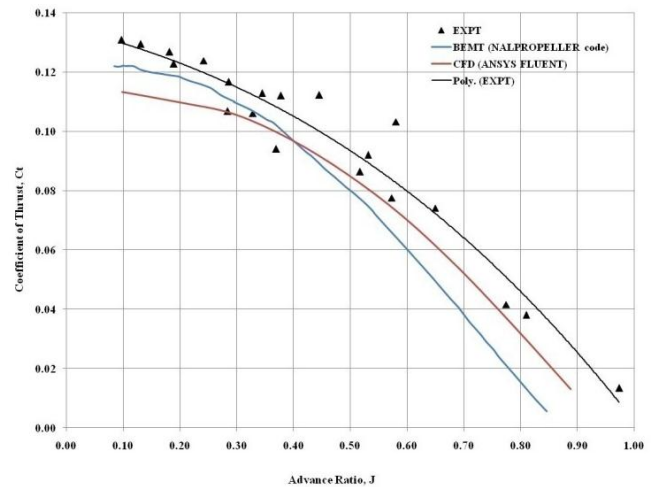


Figure 17 Coefficient of thrust vs Advance Ratio

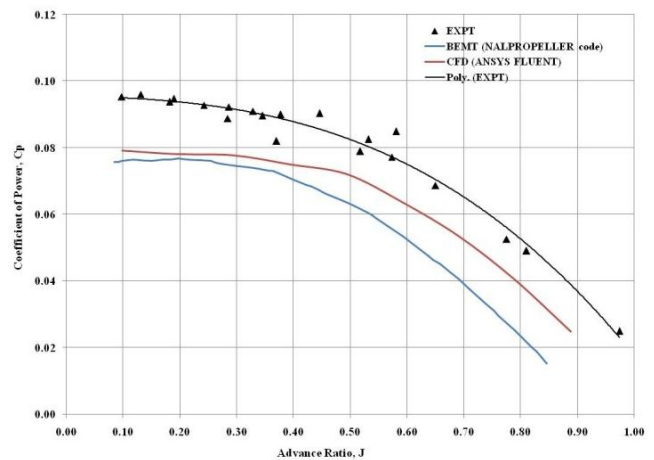


Figure 18 Coefficient of power vs Advance Ratio

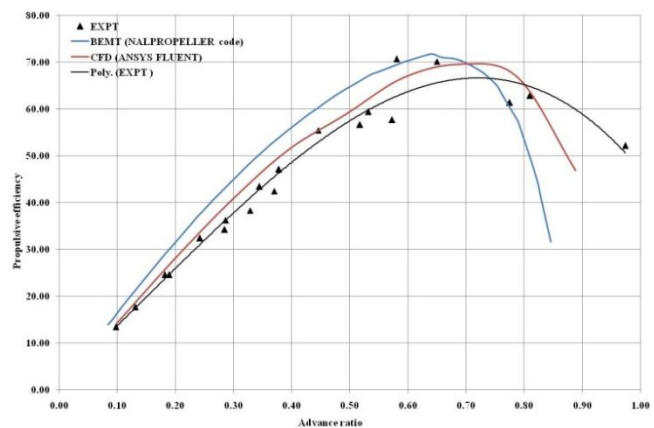


Figure 19 Propulsive efficiency vs Advance Ratio

Prediction using ANSYS FLUENT shows better comparison with that of experimental results in comparison to NALPROPELLER code. Here also, the prediction is lower than the experimental results. Grid independence study and convergence criteria did not show any appreciable deviations.

Though the exact reason could not be ascertained at this point of time, CFD sensitivity studies may show valid reason for the deficiency. From **Figure 19**, propulsive efficiencies based on coefficients of thrust, torque, and advance ratios shows better agreement with that of ANSYS FLUENT in comparison to NALPROPELLER code. The peak efficiency of 70 % is very close to operating range of advance ratios of MAV at cruise.

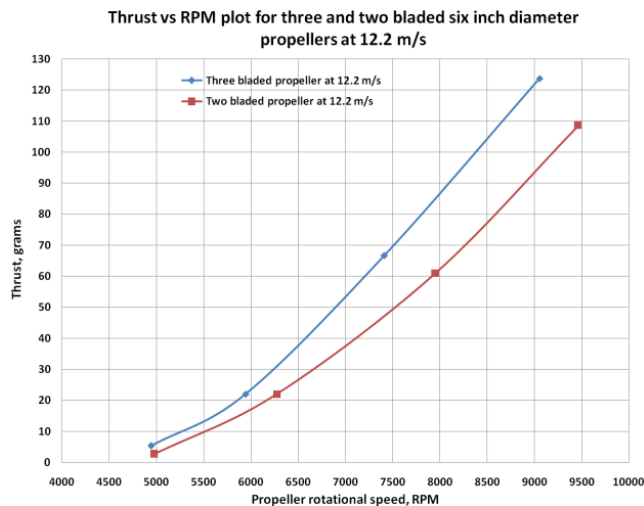


Figure 20 Thrust vs RPM

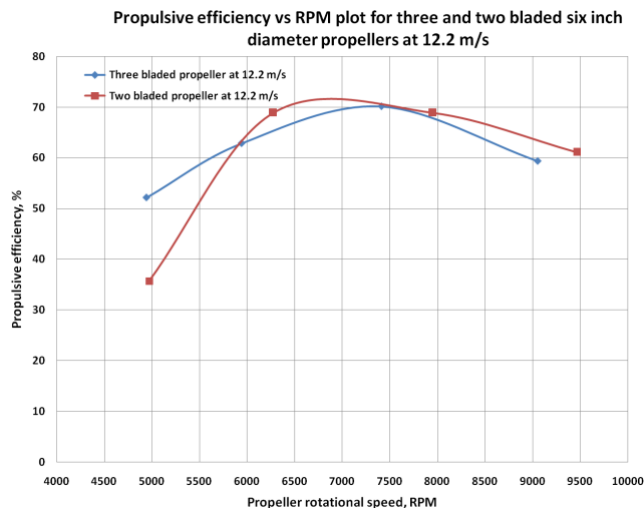


Figure 21 Propulsive efficiency vs RPM

Figure 20 and **Figure 21** shows thrust versus RPM and Propulsive efficiency versus rpm for 2-bladed and 3-bladed propellers respectively at close to design operating condition. From these figures, it can be observed that thrust at operating point (8000 rpm) for 3-bladed propeller is 88 grams, increased by 45% (as expected) compared to 2-bladed propeller (60 grams). The efficiency of 3-bladed propeller is 68% at very close to the operating advance ratios of MAV at cruise, whereas 2-bladed propeller is close to 69%. The CFRP 3-bladed propeller weighs 5.5 grams whereas the 2-bladed CFRP propeller weighs 4.6 grams.

V. CONCLUSION

The computer program developed at NAL using MATLAB is used extensively to obtain the design detail (plan form) and performance of the mini propellers viewed in multiple windows

simultaneously. Though the efficiencies of three-bladed propellers are slightly lower than the two-bladed propellers, the thrust requirement has been achieved without much penalty on weight. Structural analysis carried out shows that the maximum stresses are well within the limit of ultimate stresses of the material. The fabrication methodology adopted to realize the product with CFRP material and injection molding process is an achievement considering the size, thickness of the airfoil, and geometry of the propellers with fairly good accuracy and structural integrity.

ACKNOWLEDGMENTS

The authors wish to acknowledge NPMICAV-ADE for sponsoring this project. Authors also wish to acknowledge the support given by Director, CSIR-NAL, Head, Propulsion, MAV Division, Propulsion workshop, Propulsion drawing office and CSMST Division for completing this work.

REFERENCES

- [1] Grasmeyer, J.M and Keennon, M.T, "Development of the Black Widow micro air vehicle", Simi Valley: AeroVironment, Inc, 2001. AIAA-2001-0127.
- [2] S.J.Krishna Murthy, R.Prathapanayaka, N.Vinod Kumar, Hari Krishna.N, Jyotsana.M.Shrama, JayantLavhe, "Design and Development of Propeller for NAL Micro Air Vehicle" NAL Bangalore, NAL-PD-PR-0914, May 2009.
- [3] R. Prathapanayaka, N. Vinod Kumar, Mohan Kumar K, Hari Krishna.N R. Loganathan, S.J. Krishna Murthy "Design and Development of Propeller for NAL-Micro Air Vehicle. Part II: Performance Evaluation of Indigenous Propellers (NAL-MAV-PR01)" NAL Bangalore, PD-PR-1004, April 2010.
- [4] R. Prathapanayaka, N Vinod Kumar, Payal Agarwal, Hari Krishna N, S.J. Krishna Murthy, "CFD Analysis of Micro Air Vehicle Propellers" NAL, Bangalore, Project Document NAL-PD-PR-1008, August 2010.
- [5] R. Prathapanayaka, N.Vinod Kumar, Roshan Antony, Narendra Sharma, Varun Kumar*, Hari Krishna.N*, Bharath.D.V*, S.J.Krishna Murthy** "Experimental evaluation of Mini Propeller-Motor combinations for MAVs" NAL Bangalore, NAL-PD-PR-1108, July 2011.
- [6] R. Prathapanayaka, N Vinod Kumar, Payal Agarwal, S.J. Krishna Murthy, "CFD Analysis of Micro Air Vehicle Propeller", 13th AeSI Annual CFD Symposium, IISc, Bangalore, CP-19, August 2011.
- [7] R. Prathapanayaka, N Vinod Kumar, S.J. Krishna Murthy, "Design, Analysis, Fabrication and Testing of Miniature Propeller for MAVs", 5th Symposium on Applied Aerodynamics and Design of Aerospace Vehicles, Bangalore, P-061, G 08, Nov 2011.
- [8] Larrabee, EE. "Practical design of minimum induced loss propellers", SAE Technical Paper 790585, 1979.
- [9] MAGTROL customized propeller test setup user manual.
- [10] R. Prathapanayaka, N Vinod Kumar, S.J. Krishna Murthy, N Harikrishna, "Design and Analysis software for Propellers", ASME GTINDIA 2013, Bangalore, India, December 2013.
- [11] www.top-flite.com
- [12] N. Baldock and M.R. Mokhtarzadeh-Dehghan, "A Study of high-powered, high-altitude unmanned aerial vehicles" Aircraft engineering and Aerospace Technology: An International Journal 78 ISS, 3 (2006), Page 187-193.
- [13] ANSYS WORKBENCH 14.5 user manual, Published by ANSYS Inc, USA.
- [14] R. Prathapanayaka, N. Vinod kumar, S.J.Krishna murthy "Design and development of three bladed propeller for micro air vehicles" ICIUS-2013-69, 9th International Conference on Intelligent Unmanned Systems, Jaipur, India, September 2013.
- [15] "Mechanical Properties of carbon Fibre Composites Materials" [online] [VIEW ITEM](#)